DCT-BASED IMAGE UP-SAMPLING USING ANCHORED NEIGHBORHOOD REGRESSION

Kwok-Wai Hung, Jianmin Jiang, Qinglong Chang, Xu Wang

College of Computer Science and Software Engineering, Shenzhen University

ABSTRACT

Down-sampling in the discrete cosine transform (DCT) domain is preferable for images coded by DCT transform, such as JPEG/MJPEG/H.264, etc. Recent researches show that the truncated high-frequency DCT coefficients during the DCT down-sampling process can be estimated by learning the correlations between low-frequency and high-frequency DCT coefficients. In this paper, we propose to utilize the powerful super-resolution framework using sparse dictionaries with anchored neighborhood regression to significantly improve the accuracy of the estimated high-frequency DCT coefficients. Experimental results show that the proposed framework outperforms the state-of-the-art DCT-based up-sampling methods in terms of PSNR (0.3-1.63dB) and SSIM values for standard image datasets Set5 and Set14, while the computational time of the proposed method is 23× times faster than the state-of-the-art learning-based method using *k*-NN MMSE due to pre-computation of the ridge regression during the training process.

***Index Terms*—** DCT up-sampling, interpolation, super-resolution, ridge regression

1. INTRODUCTION

Image/video up-sampling, interpolation, super-resolution [1-4] are popular research topics due to wide applications, such as virtual reality, video coding [5-6], scalable video coding [7-9], error concealment [10], video zooming, surveillance, etc. For example, due to limited bandwidth and cost of hardware, low resolution image/video contents such as 720P or 1080P are required to up-sample to 4k resolutions in order to be displayed on the 4k displays.

In the past decades, images and videos are often coded using the block-based discrete cosine transform (DCT) in order to de-correlate image signals for better compression efficiency, such as JPEG, MJPEG, H.264, etc. Hence, a large amount of researches were devoted to investigate the direct image resolution resizing in the DCT domain [11-20]. The most efficient way to resize the images in the DCT domain is to directly truncate (discard) the high-frequency DCT coefficients for down-sampling and append zeros as the high-frequency DCT coefficients for up-sampling.

Down-sampling in the DCT domain is a simple process which simultaneously performs anti-aliasing filtering and down-sampling. Several analyses show that down-sampling in the DCT domain results in good anti-aliasing performance (narrow transition band near the Nyquist frequency) and excellent preservation of energy [9, 12-13]. Due to these reasons, many up-sampling algorithms were developed to restore the high frequency DCT coefficients from the low-resolution image down-sampled in the DCT domain [20-26].

In this paper, we propose to make use of the A+ super-resolution framework [3-4] that utilizes sparse dictionaries [27-28] and ridge regression to estimate the truncated high-frequency DCT coefficients for images down-sampled in the DCT domain. Compared with the state-of-the-art adaptive *k*-NN MMSE estimation [26], the proposed method requires several orders lower computations with higher objective and subjective quality. Specifically, training image patches are used to build the sparse dictionaries in the spatial domain using the KSVD algorithm [28]. After that, the ridge regression is used by searching for the nearest anchored neighborhood to pre-compute sets of ridge regressions. Our method is different from the original A+ super-resolution framework [3-4] in the sense that the proposed method aims for restoring the high-frequency DCT coefficients, in order to increase the resolution of the low-resolution image.

The major contributions of this work can be summarized as follows,

(i) The proposed method utilizes the powerful super-resolution framework [3-4] to tackle the high-frequency DCT coefficients estimation in the spatial domain.

(ii) The performance of the proposed method outperforms the state-of-the-art sophisticated DCT-based up-sampling algorithms in terms of PSNR and SSIM values.

(iii) The computational cost of the proposed algorithm is several orders lower than previous state-of-the-art learning-based algorithm due to offline computation of regressions.

The rest of the organization of this paper is as follows. Section 2 gives the literature review and section 3 describes the image model for DCT down-sampling. Section 4 describes the overall framework using sparse dictionaries training and ridge regression. Section 5 shows experimental results including objective and subjective evaluations, and computational analysis. Section 6 concludes the paper.

2. LITERATURE REVIEW

A more detail review of state-of-the-art DCT-based up-sampling algorithms is given here [26]. In the literature, the up-sampling methods for low-resolution images down-sampled in the DCT domain can be classified as reconstruction-based and training-based. Reconstruction-based methods include zero appending [11-14], zero appending with overlapping [8], low-pass truncation and subband approximation [15], DCT block concatenations [16-18], ringing artifacts reduction [19], trilateral filtering [20], hybrid Wiener filter [21], frequency sparsity [22], and Zernike moments [23], etc. However, reconstruction-based methods utilize the limited information from the low-resolution image without using external information.

Recently, the training-based methods [24-26] learn the correlations between the low-resolution and high-resolution images in the spatial domain [25-26] and the DCT domain [24]. However, due to the de-correlation properties of DCT coefficients, it is nontrivial to directly estimate the high-frequency DCT coefficients in the DCT domain unless the training data are highly related to the testing data [24]. Instead, the learning-based methods that make use of adaptive *k*-NN MMSE estimations in the spatial domain [25-26] achieve sophisticated performance, i.e., PSNR 1-2dB higher than conventional methods. It shows that a large amount of training data can help to estimate the high-frequency DCT coefficients in the spatial domain.

3. IMAGE MODEL OF DCT DOWN-SAMPLEING

In this section, let us review the general down-sampling process in the DCT domain for various applications [9, 12-13]. Without loss of generality, let us define the down-sampling factor be dyadic. In the spatial domain, let us denote the original high-resolution image to be $\mathbf{X} \in \Re^{2n \times 2m}$, where n and m are the dimensions of the images. The high-resolution image is divided into image patches $\mathbf{x}_i \in \mathbf{X}$. Hence, the block-based DCT down-sampling model is formulated as

$$\mathbf{y}_i = DCT^{-1}_{8\text{x}8}(T(DCT_{8\text{x}8}(\mathbf{x}_i))) \quad (1)$$

where $\mathbf{y}_i$ represents the down-sampled low-resolution image patches, $DCT_{8\text{x}8}(.)$ represents the forward 2D 8×8 DCT transform and $T(.)$ represents the truncation, scaling and down-sampling process. By processing patch-by-patch, the down-sampled low-resolution patches forms the low-resolution image $\mathbf{y}_i \in \mathbf{Y}$. Figure 1 illustrates the down-sampling process.

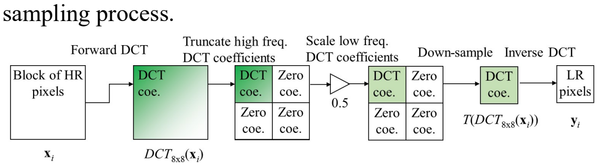

Figure 1. Dyadic DCT down-sampling process [11-14]

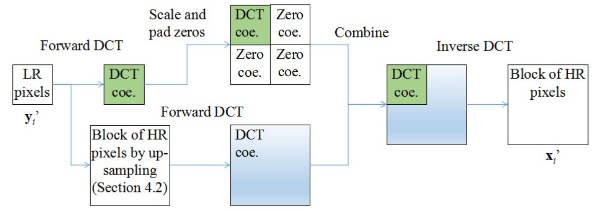

Figure 2. Overall framework of the proposed DCT up-sampling.

4. PROPOSED DCT-BASED UP-SAMPLING

In this section, we will describe the formulations of proposed DCT-based up-sampling framework.

4.1 Training process

Algorithm 1 describes the training process using sparse dictionary and ridge regression. Initially, the features of low-resolution training images were extracted using gradient and Laplacian operators and compressed using PCA projection. Then, features were coded using the KSVD algorithm [28] to generate the low-resolution sparse dictionary, as follows,

$$\mathbf{N}_l, \boldsymbol{\beta} = ksvd(PCA(F(\{\mathbf{y}_i\}))) \quad (2)$$

where $\mathbf{N}_l$ is the trained low-resolution sparse dictionary, $\boldsymbol{\beta}$ is the signal representation matrix, $F(.)$ represents the feature extraction, $PCA(.)$ represents the PCA projection, and $ksvd(.)$ represents the ksvd training [28]. The high-resolution sparse dictionary can be calculated as pseudo-inverse [3]

$$\mathbf{N}_h = (\{\mathbf{y}_i\}\boldsymbol{\beta}^T)(\boldsymbol{\beta}\boldsymbol{\beta}^T)^{-1} \quad (3)$$

where $\mathbf{N}_h$ is the generated high-resolution sparse dictionary.

The Ridge regression is then applied by searching for the K nearest anchored training samples, $\mathbf{K}_l$ and $\mathbf{K}_h$, harvested from low-resolution and high-resolution training images for each atom $\mathbf{n}_l \in \mathbf{N}_l$ of the low-resolution dictionary, as follows,

$$\hat{\mathbf{n}}_h = \mathbf{K}_h(\mathbf{K}_l^T\mathbf{K}_l + \lambda\mathbf{I})^{-1}\mathbf{K}_l^T\mathbf{n}_l = \mathbf{P}\mathbf{n}_l \quad (4)$$

where $\hat{\mathbf{n}}_h \in \mathbf{N}_h$ is the estimated atom of the high-resolution dictionary, λ is regularization parameter, and $\mathbf{P}$ is the Ridge regression that approximates the high-resolution atom.

Input: HR training patches $\{\mathbf{x}_i\}$ and LR training patches $\{\mathbf{y}_i\}$
Output: PCA projections, Ridge regressions

1. Sparse dictionaries training
   - (a) LR patches $\{\mathbf{y}_i\}$ are initially up-sampled using Bic. interpolation
   - (b) Feature extraction is used to generate $F(\{\mathbf{y}_i\})$
   - (c) PCA projection is applied to generate $PCA(F(\{\mathbf{y}_i\}))$
   - (d) K-svd algorithm [28] is adopted to generate the LR dictionary $\mathbf{N}_l$ using equation (2)
   - (e) HR dictionary $\mathbf{N}_h$ is generated by pseudo-inverse in equation (3)
2. Ridge regression
   - (a) For each atom in the low-resolution sparse dictionary $\mathbf{N}_l$,
     - (i) Search for the K nearest anchored neighborhood from LR training patches $\{\mathbf{y}_i\}$ and HR training patches $\{\mathbf{x}_i\}$
     - (ii) Compute the Ridge regression using equation (4)

Algorithm 1: Sparse dictionary training and ridge regression

Input:	LR testing patch $\mathbf{y}_i$', PCA projections, Ridge regressions
Output:	Estimated HR testing patch $\mathbf{x}_i$'

1. Feature extractions and PCA projections
   (a) LR patch $\mathbf{y}_i$' is initially up-sampled using Bicubic interpolation
   (b) Feature extraction is used to generate $F(\mathbf{y}_i')$
   (c) PCA projection is applied to generate $PCA(F(\mathbf{y}_i'))$
2. Search for Ridge regression
   (a) Projected PCA feature $PCA(F(\mathbf{y}_i'))$ is used to search for the nearest atom $\mathbf{n}_{l,j}$ in the LR sparse dictionary $\mathbf{N}_l$
   (b) Use the corresponding Ridge regression $\mathbf{P}_j$ to obtain the up-sampled HR patch $\mathbf{x}_i'=\mathbf{P}_j(PCA(F(\mathbf{y}_i')))$
3. Refine low-frequency DCT coefficients
   (a) DCT transform of both LR patch $\mathbf{y}_i$' and up-sampled HR patch $\mathbf{x}_i$' to generate $DCT_{8x8}(\mathbf{y}_i')$ and $DCT_{8x8}(\mathbf{x}_i')$
   (b) Refine the low-frequency DCT coefficients of the up-sampled HR patch using equation (8)
   (c) Inverse DCT transform to obtain the final estimated HR patch $\mathbf{x}_i$' using equation (9)

Algorithm 2: DCT up-sampling process using ridge regression

4.2 Up-sampling process with refinement

Algorithm 2 shows the up-sampling process for a given low-resolution image patch from the down-sampled low-resolution image. Initially, the low-resolution patch $\mathbf{y}_i$' is up-sampled using Bicubic interpolation and feature extraction is applied to generate the input feature for the PCA projection, $PCA(F(\mathbf{y}_i'))$. After that, projected feature is used to search for the nearest atom in the low-resolution sparse dictionary,

$$j = \min_j \left\| PCA(F(\mathbf{y}_i^{'}) - \mathbf{n}_{l,j} \right\|_2^2 \quad \text{for } \mathbf{n}_{l,j} \in \mathbf{N}_l \tag{5}$$

where j represents the index of the atom which has the lowest Euclidean distance to projected feature $PCA(F(\mathbf{y}_i'))$. Hence, the corresponding Ridge Regression $\mathbf{P}_j$ (computed during the training process) is applied to up-sample the low-resolution patch $\mathbf{y}_i$' as follows,

$$\mathbf{x}_i^{'} = \mathbf{P}_j PCA(F(\mathbf{y}_i^{'}) \tag{6}$$

where the up-sampled HR patch $\mathbf{x}_i$' will be further improved by fitting the down-sample model in (1). Then, forward DCT transform is applied to the up-sampled HR patch $\mathbf{x}_i$' and LR patch $\mathbf{y}_i$' to refine the low-frequency DCT coefficients [26],

$$\mathbf{x}_i^{'} = \min_{\mathbf{x}_i^{'}} \left\| T(DCT_{8\text{x}8}(\mathbf{x}_i^{'})) - DCT_{8\text{x}8}(\mathbf{y}_i^{'}) \right\|_2^2 \tag{7}$$

where the closed-form solution of equation (7) is to subtract the difference between the low-frequency DCT coefficients of the up-sampled HR patch $\mathbf{x}_i$' and the LR patch $\mathbf{y}_i$',

$$DCT_{8\text{x}8}(\mathbf{x}_i^{'}) - T^{-1}(T(DCT_{8\text{x}8}(\mathbf{x}_i^{'})) - DCT_{8\text{x}8}(\mathbf{y}_i^{'})) \tag{8}$$

and apply the inverse DCT transform to obtain the final result of the estimated HR patch $\mathbf{x}_i$', as follows,

$$\mathbf{x}_i^{'} = DCT_{8\text{x}8}^{-1}\left(DCT_{8\text{x}8}(\mathbf{x}_i^{'}) - T^{-1}(T(DCT_{8\text{x}8}(\mathbf{x}_i^{'})) - DCT_{8\text{x}8}(\mathbf{y}_i^{'}))\right) \tag{9}$$

where $DCT_{8\text{x}8}^{-1}(.)$ represents the inverse 2D 8×8 DCT transform and $T^{-1}(.)$ represents the zero appending, scaling and up-sampling process in the DCT domain. By refining the low-frequency DCT coefficients, the up-sampling process essentially estimates the high-frequency DCT coefficients.

5. EXPERIMENTAL RESULTS

Extensive experiments were done to evaluate the performance of the proposed method in terms of objective and subjective measurements and computational time. The system for experiment was an Intel i7 3.4 GHz PC with 32G memory using MATLAB as the coding language. The state-of-the-art DCT-based up-sampling methods for comparison include the Bicubic interpolation, zero appending [11-14], zero appending with overlapping [8], hybrid Wiener filter [21], and adaptive k-NN MMSE estimation [26].

Without the loss of generality, the down-sampling and up-sampling factor is two. For a fair comparison, the standard CVPR08-91 dataset [2] that comprises of 91 images were used as the training data for adaptive k-NN MMSE estimation [26] and the proposed method. For the testing data, the datasets, Set5 and Set14 [27], were used.

5.1 Parameters settings

For the parameters settings, the number of ridge regressions (dictionary sizes) is 8192, and the number of training patches extracted from the HR training images is 20 million. Figure 3 shows the changes of PSNR values against computational times with respect to the number of regressions. Due to diminishing increase of PSNR values with computational time, the current settings were chosen.

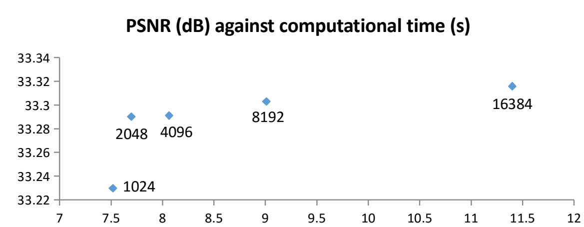

Figure 3. PSNR values (y-axis) against computational time (x-axis) with respect to the number of regressions in range [1024, 16384]

5.2 Computational time

Table 1 shows the computational time of the several DCT-based up-sampling methods, and the proposed method. Specifically, the proposed method requires 23 times lower computational time than the state-of-the-art adaptive k-NN MMSE estimation [26] due to the pre-computation of ridge regression during the training process.

Table 1. Computational time (s) of DCT up-sampling methods

Bicubic interpolation	Zero append [11-14]	Zero append overlap [8]	Hybrid WF [21]	Adaptive k-NN [26]	Proposed method
0.13	0.18	0.74	0.17	208.26	9.01

Table 2. PSNR (dB) and SSIM values of different DCT up-sampling methods and the proposed method

Set5 Set14	**PSNR (dB) and SSIM (highest values are bolded)**											
	Bicubic interpolation		**Zero append [11-14]**		**Zero append over. [8]**		**Hybrid WF [21]**		**Adaptive *k*-NN [26]**		**Proposed method**	
baboon	24.87	0.7183	25.11	0.7453	25.07	0.7399	25.01	0.7434	25.38	0.7593	**25.47**	**0.7628**
baby_GT	37.51	0.9570	37.67	0.9595	37.85	0.9610	37.83	0.9604	38.39	0.9643	**38.57**	**0.9655**
barbara	28.11	0.8518	28.35	0.8636	28.25	0.8615	28.14	0.8628	28.42	0.8720	**28.59**	**0.8769**
bird_GT	37.39	0.9755	37.41	0.9732	37.99	0.9780	38.08	0.9764	40.50	0.9853	**41.18**	**0.9869**
bridge	26.79	0.8103	26.98	0.8259	27.06	0.8276	26.92	0.8255	27.53	0.8443	**27.68**	**0.8483**
butterfly_GT	27.99	0.9220	28.03	0.9128	28.49	0.9261	28.55	0.9186	31.51	0.9592	**32.08**	**0.9638**
coastguard	29.55	0.8129	29.66	0.8284	29.97	0.8340	29.62	0.8317	30.56	0.8468	**30.63**	**0.8482**
comic	26.51	0.8675	26.65	0.8739	26.96	0.8819	26.74	0.8755	28.05	0.9080	**28.33**	**0.9146**
face	35.08	0.8710	35.23	0.8795	35.29	0.8783	35.28	0.8796	35.62	0.8852	**35.69**	**0.8869**
flowers	30.82	0.9079	30.94	0.9105	31.25	0.9162	31.11	0.9120	32.69	0.9313	**33.09**	**0.9360**
foreman	33.21	0.9554	33.78	0.9577	33.57	0.9581	34.13	0.9558	35.49	0.9684	**35.73**	**0.9704**
head_GT	35.12	0.8700	35.31	0.8788	35.33	0.8772	35.33	0.8783	35.65	0.8838	**35.73**	**0.8856**
lenna	35.14	0.9166	35.24	0.9203	35.53	0.9214	35.44	0.9200	36.45	0.9278	**36.63**	**0.9291**
man	29.54	0.8562	29.70	0.8641	29.80	0.8659	29.73	0.8637	30.63	0.8816	**30.82**	**0.8854**
monarch	33.51	0.9634	33.54	0.9614	34.01	0.9655	33.98	0.9630	36.61	0.9749	**37.24**	**0.9768**
pepper	33.44	0.9089	33.89	0.9087	33.68	0.9107	33.38	0.9061	35.52	0.9195	**35.82**	**0.9205**
ppt3	27.41	0.9502	27.61	0.9426	27.90	0.9519	27.83	0.9428	29.79	0.9732	**30.32**	**0.9779**
woman_GT	32.62	0.9525	32.76	0.9527	33.11	0.9566	32.81	0.9523	34.87	0.9679	**35.21**	**0.9691**
zebra	31.28	0.9215	31.51	0.9280	31.83	0.9312	31.77	0.9294	33.41	0.9405	**33.84**	**0.9438**
Average	31.36	0.8941	31.55	0.8993	31.73	0.9023	31.67	0.8999	33.00	0.9154	**33.30**	**0.9183**

5.3 PSNR and SSIM comparisons

Image datasets Set5 and Set14 [27] were used to evaluate the performance of several DCT-based up-sampling methods. Table 2 shows the PSNR and SSIM values of 19 images from Set5 and Set14. On average, the proposed method outperforms the adaptive *k*-NN MMSE method [26] by 0.3 dB in PSNR with 23.1 times lower computational time, and Hybrid Wiener filter [21] by 1.63 dB in PSNR.

Figure 4 and Figure 5 show the subjective comparisons of several up-sampling methods, which show that the proposed method provides better subjective quality than other state-of-the-art methods. Specifically, the edges and textures of the proposed method are clearer and sharper with higher fidelity. Moreover, the proposed method produces less staircase and ringing artifacts among all methods. Subjective evaluations generally agree with the objective measurements in Table 2.

Zero append [11-14] **Adaptive *k*-NN [26]** **Proposed method** **Original HR image**

Figure 4. Subjective comparisons of DCT up-sampling methods

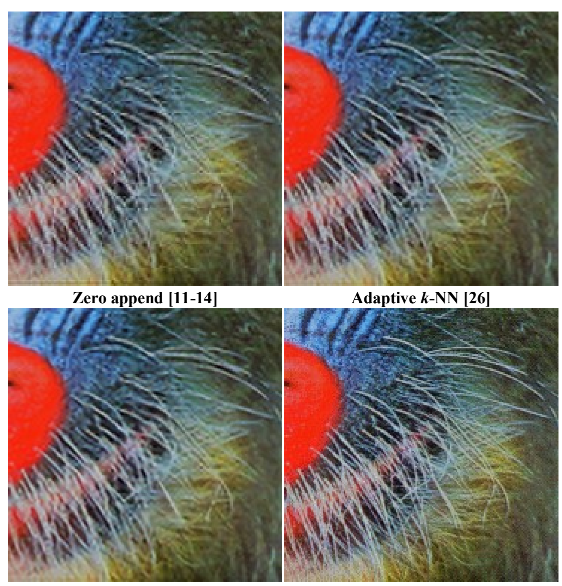

Proposed method **Original HR image**

Figure 5. Subjective comparisons of DCT up-sampling methods.

6. CONCLUSION

In this paper, we propose a new DCT-based up-sampling method for images down-sampled in the DCT domain. Specifically, the major contribution of this paper is to achieve the new state-of-the-art results by using anchored neighborhood regression with the sparse dictionaries to estimate the high-frequency DCT coefficients in the spatial domain. More importantly, the computational costs of the proposed method is several orders lower than previous state-of-the-art learning-based DCT up-sampling method due to pre-computation of the regressions in the training process. Experimental results show that the subjective and objective quality of the proposed method outperforms the existing state-of-the-art DCT-based up-sampling methods.

Acknowledgement: This work was supported in part by the Shenzhen Emerging Industries of the Strategic Basic Research Project (No. JCYJ20160226191842793), and the National Natural Science Foundation of China (No. 61602312, 61620106008).

7. REFERENCES

[1] Kwok-Wai Hung and Wan-Chi Siu, "Robust soft-decision interpolation using weighted least squares," *IEEE Transactions on Image Processing*, vol.21, no.3, pp.1061-1069, March 2012.

[2] Jianchao Yang, John Wright, Thomas Huang, and Yi Ma, “Image super-resolution as sparse representation of raw image patches”, *IEEE Computer Society Conference on Computer Vision and Pattern Recognition (CVPR 2008)*, June 2008, US

[3] R. Timofte, V. De Smet, and L. Van Gool, “A+: Adjusted Anchored Neighborhood Regression for Fast Super-Resolution.” *Asian Conference on Computer Vision (ACCV 2014)*, November 2014, Singapore.

[4] R. Timofte, R. Rothe, and L. Van Gool, “Seven ways to improve example-based single image super resolution” *IEEE Computer Society Conference on Computer Vision and Pattern Recognition (CVPR 2016)*, June 2016, US

[5] Minmin Shen, Ping Xue and Ci Wang, "Down-Sampling Based Video Coding Using Super-Resolution Technique," *IEEE Transactions on Circuits and Systems for Video Technology*, vol.21, no.6, pp.755-765, June 2011

[6] X. Wu, X. Zhang and X. Wang, "Low bit-rate image compression via adaptive down-sampling and constrained least squares upconversion", *IEEE Transactions on Image Processing*, vol. 18, no. 3, pp. 552-561, Mar. 2009.

[7] Z. Shi, X. Sun, F. Wu, "Spatially Scalable Video Coding For HEVC," *IEEE Transactions on Circuits and Systems for Video Technology*, vol.22, no.12, pp.1813-1826, Dec. 2012

[8] IlHong Shin and Hyun Wook Park, "Adaptive Up-Sampling Method Using DCT for Spatial Scalability of Scalable Video Coding," *IEEE Transactions on Circuits and Systems for Video Technology*, vol.19, no.2, pp.206-214, Feb. 2009

[9] Haiyan Shu and Lap-Pui Chau, "A Resizing Algorithm With Two-Stage Realization for DCT-Based Transcoding," *IEEE Transactions on Circuits and Systems for Video Technology*, vol.17, no.2, pp.248-253, Feb. 2007

[10] Z. Alkachouh and M.G. Bellanger, "Fast DCT-based spatial domain interpolation of blocks in images," *IEEE Transactions on Image Processing*, vol.9, no.4, pp.729-732, Apr 2000

[11] K. N. Ngan, “Experiments on two-dimensional decimation in time and orthogonal transform domains,” *Signal Processing*, vol. 11, pp. 249–263, 1986.

[12] YoungSeo Park and HyunWook Park, "Design and analysis of an image resizing filter in the block-DCT domain," *IEEE Transactions on Circuits and Systems for Video Technology*, vol.14, no.2, pp. 274- 279, Feb. 2004

[13] R. Dugad and N. Ahuja, “A fast scheme for image size change in the compressed domain,” *IEEE Transactions on Circuits and Systems for Video Technology*, vol. 11, no. 4, pp. 461–474, Apr. 2001.

[14] Ci Wang, Hong-Bin Yu and Meng Zheng, "A fast scheme for arbitrarily resizing of digital image in the compressed domain," *IEEE Transactions on Consumer Electronics*, vol.49, no.2, pp. 466- 471, May 2003

[15] J. Mukherjee and S.K. Mitra, "Image resizing in the compressed domain using subband DCT," *IEEE Transactions on Circuits and Systems for Video Technology*, vol.12, no.7, pp.620-627, Jul 2002

[16] Young Seo Park and Hyun Wook Park, "Arbitrary-ratio image resizing using fast DCT of composite length for DCT-based transcoder," *IEEE Transactions on Image Processing*, vol.15, no.2, pp.494-500, Feb. 2006

[17] C. Salazar and T.D. Tran, "A Complexity Scalable Universal DCT Domain Image Resizing Algorithm," *IEEE Transactions on Circuits and Systems for Video Technology*, vol.17, no.4, pp.495-499, April 2007

[18] V. Patil, R. Kumar and J. Mukherjee, "A Fast Arbitrary Factor Video Resizing Algorithm," *IEEE Transactions on Circuits and Systems for Video Technology*, vol.16, no.9, pp.1164-1171, Sept. 2006

[19] Hyungjun Lim and H. Park, "A Ringing-Artifact Reduction Method for Block-DCT-Based Image Resizing," *IEEE Transactions on Circuits and Systems for Video Technology*, vol.21, no.7, pp.879-889, July 2011

[20] Zhenyu Wu, and Hong Hu, “Trilateral Filtering-based Hybrid Up-sampling in Dual Domains for Single Video Frame Super Resolution”, *IEEE International Conference on Image Processing (ICIP 2016)*, pp. 1160-1164, Sept 2016, US

[21] Zhenyu Wu, Hongyang Yu and Chang Wen Chen, "A New Hybrid DCT-Wiener-Based Interpolation Scheme for Video Intra Frame Up-Sampling," *IEEE Signal Processing Letters*, vol.17, no.10, pp.827-830, Oct. 2010

[22] Meng Zhang, Tinghuan Chen, Xuchao Shi, and Peng Cao, “Image Arbitrary-Ratio Down- and Up-Sampling Scheme Exploiting DCT Low Frequency Components and Sparsity in High Frequency Components”, *IEICE Trans. Inf. & Syst.*, vol. E99-D, no. 2, pp. 475-487, February 2016

[23] Chandan Singh, and Ashutosh Aggarwal, “A comparative performance analysis of DCT-based and Zernike moments-based image up-sampling techniques”, *Optik*, vol. 127, Issue 4, pp. 2158-2164, February 2016

[24] Min-Kyoung Cho and Byung-Uk Lee, "Discrete cosine transform domain image resizing using correlation of discrete cosine transform coefficients", *Journal of Electronic Imaging* 15(3), 033009 (Jul–Sep 2006)

[25] Kwok-Wai Hung, Wan-Chi Siu, "Block-Adaptive DCT-Wiener Image Up-Sampling", *IEEE Int. Conf. Acoustics, Speech, Signal Processing (ICASSP 2014)*, pp.5809-5813, 4-9 May 2014, Florence, Italy.

[26] Kwok-Wai Hung, and Wan-Chi Siu, “Novel DCT-Based Image Up-sampling using Learning-Based Adaptive k-NN MMSE Estimation, “*IEEE Transactions on Circuits and Systems for Video Technology*, vol. 24, no. 12, pp. 2018–2033, Dec. 2014

[27] Zeyde, R., Elad, M., Protter, M., “On Single Image Scale-Up Using Sparse-Representations.” *Curves and Surfaces*, pp.711-730, 2012

[28] Michal Aharon, Michael Elad, and Alfred Bruckstein, “K-SVD: An Algorithm for Designing Overcomplete Dictionaries for Sparse Representation”, *IEEE Transactions on Signal Processing*, vol. 54, no. 11, Nov 2006.